93 GHz Wireless Transmission based on a Fully Packaged mm-Wave Band Optical Clock Generator

Alberto Montanaro
Photonic Networks and Technologies National Lab (PNTLab)
National Inter-University Consortium for Telecommunications (CNIT)
Pisa, Italy
ORCID: 0000-0002-2844-0433

Claudio Porzi
Telecommunications, Computer Engineering, and Photonics Institute (TeCIP)
Scuola Superiore Sant'Anna
Pisa, Italy
claudio.porzi@santannapisa.it

Fawad Ahmad
Telecommunications, Computer Engineering, and Photonics Institute (TeCIP)
Scuola Superiore Sant'Anna
Pisa, Italy
Fawad.Ahmad@santannapisa.it

Marco Chiesa
CamGraPhIC s.r.l.
Pisa, Italy
Marco.Chiesa@camgraphic-technology.com

Antonio D'Errico
Ericsson Research
Pisa, Italy
antonio.d.errico@ericsson.com

Alessandra Bigongiari
Ericsson Research
Pisa, Italy
alessandra.bigongiari@ericsson.com

Aina Serrano Rodrigo
CamGraPhIC s.r.l.
Pisa, Italy
Aina.Serrano.Rodrigo@camgraphic-technology.com

Federico Camponeschi
Telecommunications, Computer Engineering, and Photonics Institute (TeCIP)
Scuola Superiore Sant'Anna
Pisa, Italy
federico.camponeschi@santannapisa.it

Marco Romagnoli
Photonic Networks and Technologies National Lab (PNTLab)
National Inter-University Consortium for Telecommunications (CNIT)
Pisa, Italy
marco.romagnoli@cnit.it

Antonella Bogoni
Telecommunications, Computer Engineering, and Photonics Institute (TeCIP)
Scuola Superiore Sant'Anna
Pisa, Italy
antonella.bogoni@santannapisa.it

Antonio Malacarne
Photonic Networks and Technologies National Lab (PNTLab)
National Inter-University Consortium for Telecommunications (CNIT)
Pisa, Italy
ORCID: 0000-0002-8240-2171

2023 International Topical Meeting on Microwave Photonics (MWP) | 979-8-3503-4221-5/23/$31.00 ©2023 IEEE | DOI: 10.1109/MWP58203.2023.10416604

***Abstract*— The mm-wave frequency spectrum offers the possibility to afford the increasing demand of high data-rate communication links. Microwave-photonics techniques can be advantageously used for reconfigurable generation of very high frequency clocks with superior phase noise performance with respect to purely electrical techniques, with the additional functionality of remote distribution of the signal through fiber-optics or free-space optic links. Here we present a fully packaged optoelectronic assembly of a CMOS-compatible silicon-based photonic integrated circuit for optical frequency comb generation with reconfigurable free spectral range given by an RF driving local oscillator. Through optical filtering and photodetection, a 98 GHz electrical clock has been derived and employed for successful 93 GHz wireless transmission of complex modulation formats carrying up to 4 Gb/s data rate, demonstrating the suitability of the solution for 5G and next generation 6G mobile networks.**

Keywords—Microwave photonics, Integrated microwave photonics, mm-wave, 6G technology, sub-THz generation, optoelectronic packaging, wireless communications.

I. Introduction

The next 5G new radio (NR) and 6G wireless technologies are expected to afford the demand of high data-rate links, low-latency networks with maximized number of connected devices to enable new applications such as digital twins, AI computing, remote surgery etc.[1]-[3]. To this end, novel hardware operating in the sub-THz range, allowing low phase noise, high signal integrity at > 100 GHz carrier frequency, and tens of Gbit/s channel capacity will be necessary [4],[5]. As the operating frequency increases, standard electronics shows its limits in terms of phase noise and signal integrity [6]. For these reasons, microwave photonics techniques can be advantageously used to overcome these issues [7]. Indeed, ultra-wide bandwidth operation, wide tuneability and extremely stable radio-frequencies generation can be achieved using optical techniques. For example, frequency combs coupled to ultrafast unitravelling-carrier photodiodes have been used to demonstrate the generation of sub-THz frequencies up to 300 GHz exhibiting phase noise (PN) as low as 100 dBc/Hz at 10 kHz [8]. In addition, with respect to standard BiCMOS-based solutions [9], optical generation of high-frequency reference clocks enables their efficient distribution over low-loss and electromagnetic interference (EMI)-free fiber-optics or free-space optic links [10]-[12]. System miniaturization through a suitable integration technology and packaging strategy is regarded as a further step for making photonics-based RF synthesizers a viable alternative to electronics devices, therefore enabling its exploitation in several practical environments [7],[13].

Recent achievements demonstrated the effectiveness of silicon photonics (SiP) solutions for reconfigurable frequency multiplication of radiofrequency oscillations in the gigahertz range, up to W-band and beyond, with phase noise performance in line with ideal frequency multipliers [14],[15]. The approach is based on optoelectronic modulation-based

This work was partially supported by the EU under the Italian National Recovery and Resilience Plan (NRRP) of NextGenerationEU, partnership on "Telecommunications of the Future" (PE00000001 – program "RESTART"), and by the Italian Ministry of University and Research through the COSMOS project (grant number FISR2019_0347).

optical frequency comb (OFC) generation and optical bandpass filtering.

Here we present a W-band optical clock generation based on a miniaturized functionally packaged silicon-based photonic integrated circuit (PIC) for OFC generation with adjustable free spectral range (FSR). The optoelectronic package includes a printed circuit board (PCB) for feeding the PIC with the necessary DC signals and an RF local oscillator operating over a wide frequency range of about 8 GHz centered around 20 GHz. With proper optical filtering through a bulky commercial device, a low-phase noise mm-wave band reference clock at 98 GHz-frequency has been obtained in the optical domain and subsequent up conversion at 93 GHz of complex modulation data signals is achieved through optoelectronic modulation and photodetection through commercial devices. Wireless transmission and successful detection of data rates up to 4Gb/s has been demonstrated, proving the suitability of such approach for effective low-phase noise mm-wave band reference clock generation for B5G/6G mobile networks.

II. W-Band Optical Clock Generation

A. Optoelectronic packaging

The photonic integrated circuit (PIC) has been designed for fabrication on silicon on insulator (SOI) technology. The whole PIC embeds several structures including a carrier depletion-based SiP phase modulator (PM) that can be driven by an electrical local oscillator (LO) up to 20 GHz, whose limitation is given by the PM bandwidth response. OFC generation with FSR equal to the provided LO frequency is achieved by providing high electrical RF power to the modulator, in such a way to induce the nonlinear regime.

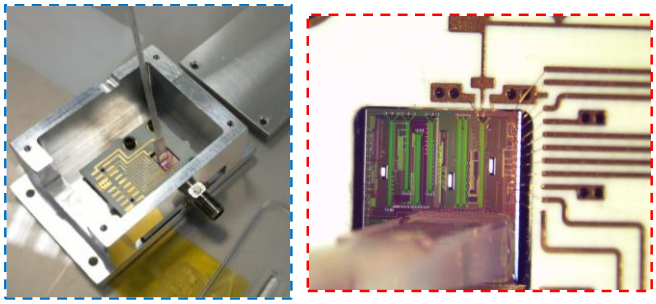

Fig. 1. The fully packaged optoelectronic device (left) and microscope picture of the PIC wire-bonded to RF and DC pads of the PCB.

Parallel to PIC fabrication, a PCB to be wedge-bonded to the PIC, carrying both the input LO reference for OFC generation and other DC control signals for different on-chip actuators including thermally tunable optical couplers/splitters for OFC generation monitoring, has been developed. Coupling of the microwave signal with the DC reverse bias of the SiP modulator pn-junction is performed through an on-board bias tee. Since the comb source benefits from driving the SiP PM with large voltage values and considering power dissipation due to RF and DC bias signals at the termination load of the traveling-wave line realized above the modulator, a custom design for the bias tee able to support power levels of up to about 1.5 W has been adopted. The matching network is designed to operate in proximity of the SiP modulator cut-off frequency, which is about 20 GHz at the typical operating reverse-bias voltage levels of 3.5 V. This allows attaining the mm-wave band with a relatively low multiplication factor of the input LO frequency, which helps in keeping the optical power of the selected OFC tones sufficiently large. A relatively broad range of about 8 GHz around this value has been also pursued for the operating frequencies, which can be advantageous for flexible selection of LO frequency or in presence of wideband modulated RF driving signals [16]. The effect of wedge-bonds has been included in the model according to [17]. Fig. 1(left) shows the fully packaged device including K connector on the PCB for LO injection and a glued fiber array for C-band optical input/output coupling. In Fig. 1(right) a microscope picture allows to appreciate the PIC-to-PCB RF and DC wedge-bonds. The package includes a Peltier cell below the PIC and an integrated thermistor on it, both bonded to PCB pads. Through an external temperature controller, temperature accuracy of ± 0.002 °C is achieved. All DC control signals are provided to the PCB through a molex connector.

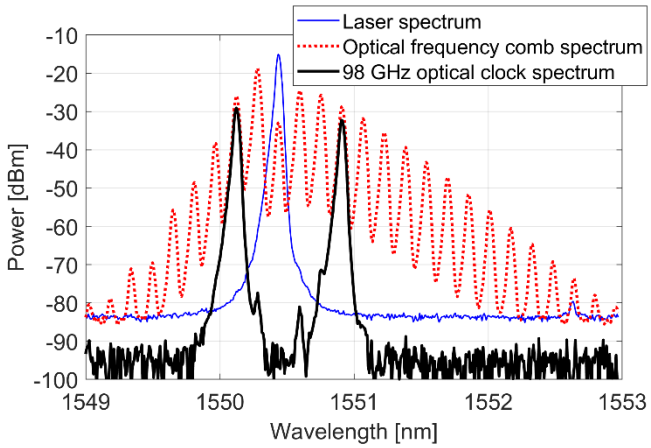

Fig. 2. Optical spectrum of the input laser, of the generated OFC and at the programmable optical filter output.

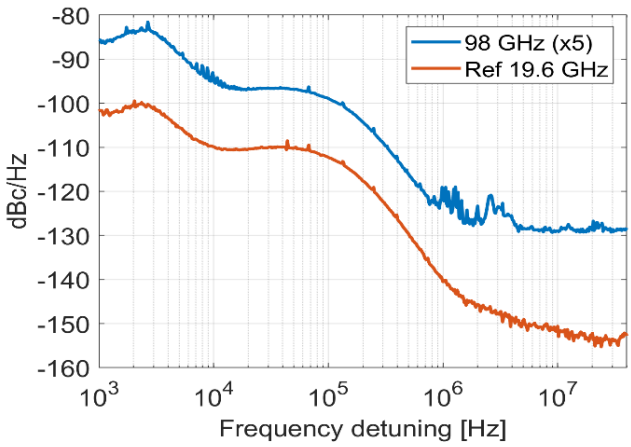

Fig. 3. Phase noise measurement in the frequency detuning range [1 kHz – 40 MHz] of the generated 98-GHz clock and the 19.6 GHz local oscillator.

B. Characterization of the W-Band Optical Clock

The described package has been used to generate a W-band (75-110 GHz) optical clock. For an LO input power of 28.5 dBm at a frequency of 19.6 GHz, Fig. 2 reports in dotted red the obtained OFC spectrum for an input laser whose spectrum is shown in thin blue. Then, through an external programmable optical filter, two 98 GHz-spaced modes (5 × 19.6 GHz) are selected, so as to obtain the thick black spectrum. Such a 98 GHz optical clock, when photo-detected with a 100 GHz photodiode, exhibits the phase noise (PN) performance plotted in Fig. 3. By comparing it with the PN of

the reference 19.6 GHz LO, the similar shape and the 14-to-15 dB difference confirm that the performance are in line with an ideal frequency multiplier. Indeed, from the curves in Fig. 3, a root mean square time jitter of 15 fs and 16.45 fs has been calculated, for the reference LO and the W-band reference clock, respectively. The small worsening in terms of time jitter is most probably due to the disturb present on the 98 GHz PN curve in the frequency detuning range 1-4 MHz and the subsequent noise floor reached for higher detuning, caused by the signal-to-noise ratio.

III. Wireless Transmission Experiment

A. Experimental Seup

The experimental setup is shown in Fig. 4. The packaged integrated comb generator is fed by an optical continuous wave (CW) laser at the wavelength of 1550 nm and driven by an electrical 19.6-GHz LO whose power is 28.5 dBm after RF amplification. A polarization controller (PC) is used to match the input polarization state with the one supported by the silicon PIC. The optical output consists of the dotted red spectrum of Fig. 2. As optical programmable filter a WaveShaper by Finisar (WS) has been employed to obtain the black spectrum of Fig. 2. The WS output has been amplified by an Erbium-doped fiber amplifier (EDFA) to compensate for input-output overall PIC loss, WS loss of 5 dB and intrinsic comb generation efficiency, and a 1 nm-wide optical bandpass filter (OBPF) is then used to remove out-of-band amplified spontaneous emission (ASE). The optical signal subsequently passes through a Mach-Zehnder modulator (MZM) driven by a data signal generated at an intermediate frequency (IF) of 5 GHz by a 64 GS/s 11 GHz digital-to-analog converted (DAC). A second PC optimizes the MZM input polarization state. The MZM output is then photo-detected by a 100-GHz photodiode and the signal term upconverted at $f_{RF} - f_{IF} = 93$ GHz, that is carrying the data, is selected by a WR10 waveguide cavity filter with passband 86-94 GHz. The signal is finally amplified by a W-band amplifier and transmitted through a 2-meter wireless link using a W-band 35-dB gain antenna. At the receiver side an identical antenna receives the signal that is down-converted back to f_{IF} thanks to a 92-96 GHz active downconverter. Antennas exhibit the same frequency range. A 40GS/s 12-GHz bandwidth real-time oscilloscope is finally used to acquire the signal and perform error vector magnitude measurements.

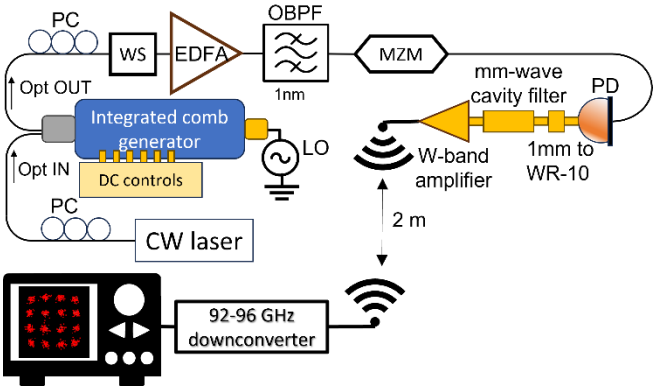

Fig. 4. Block diagram of the implemented experimental setup for W-band wireless transmission.

B. Experimental Results

The point-to-point W-band wireless transmission has been tested with complex modulation formats, i.e. quadrature phase-shift keying (QPSK) and 16-quadrature amplitude modulation (QAM). The performance of a 0.5Gbaud/s (2 Gb/s) 16-QAM transmission is detailed in Fig. 5(top), where the error vector magnitude (EVM) has been measured through a digital signal processing (DSP) tool embedded in the oscilloscope. The DSP consists in phase recovery and in the use of an equalization filter whose length has been optimized in the range 21-51 symbols, depending on the modulation format and data rate. A digital raised cosine filter is also used, with bandwidth varied according to the electrical bandwidth of the received signal. The analysis also includes constellation reconstruction and visualization of I or Q eye diagram. With the maximum available power an EVM = 6% was achieved. The same analysis is reported in Fig. 5(bottom) for a 2Gbaud (4 Gb/s) QPSK signal, with a lowest EVM measured to be 15%.

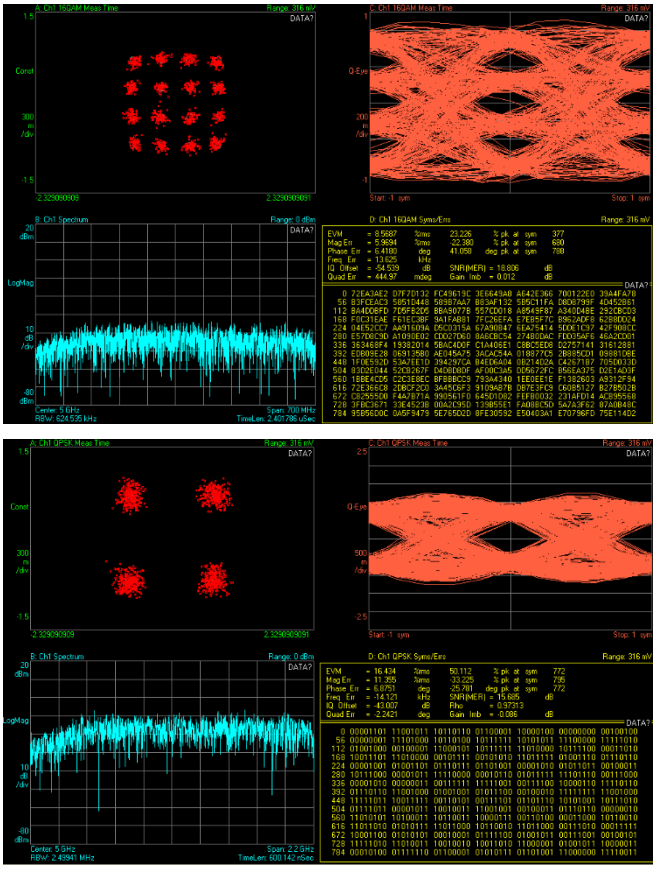

Fig. 5. Detection performance of 2 Gb/s 16-QAM (top) and 4 Gb/s QPSK (bottom) transmission with, for each, case, reconstructed eye diagram, complex constellation, spectrum at IF and EVM statistics.

A further analysis, reported by Fig. 6, has been extended to 1 Gb/s and 2 Gb/s QPSK signals, measuring the achievable EVM value as a function of the optical power reaching the PD input at the transmitter. As expected, the performance degrades for higher data rate. The quite high penalty from 2 Gb/s to 4 Gb/s QPSK is most probably caused by the bandwidth limitation imposed by the electrical chain of the employed W-band devices. The frequency range overlap of W-band filter, amplifier, antennas and down-converter is estimated to be lower than 2 GHz and not precisely centered with respect to 93 GHz. Indeed, the spectrum reported by Fig. 5(bottom) exhibits an asymmetric behavior. It is worth to notice that for 2 Gb/s 16-QAM the 11.2% EVM threshold required by the standards for ¾ code rate is achieved for optical power > -1 dBm.

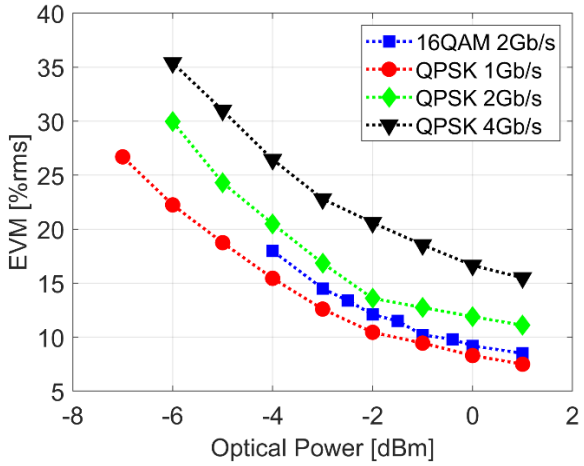

Fig. 6. Error vector magnitude measurements for QPSK and 16-QAM modulation formats versus the optical power received by the photodetector at the wireless transmitter.

IV. Conclusions and Future Perspectives

A full optoelectronic packaging of a silicon-based photonic integrated circuit (PIC) for reconfigurable optical frequency comb generation based on a pn-junction phase modulator operating in carrier depletion regime, has been realized. It comprises a PCB wedge-bonded to the PIC for DC and RF electrical signal feeding, a Peltier cell and integrated thermistor for temperature stabilization, DC feeding takes place through a Molex connector and RF driving through a K connector. The device accepts local oscillator frequencies in an 8 GHz-wide range around 20 GHz and was used to generate a low-phase noise 98 GHz optical clock, by adding an external optical filtering stage. Through subsequent optical intensity modulation and photodetection, complex data signals up to 4 Gb/s QPSK and 2 Gb/s 16-QAM have been successfully up-converted at the 93-GHz carrier frequency and transmitted over a 2-meter-long wireless link. EVM measurements confirm the effectiveness of the proposed optical clock generator that can, in principle, reach output frequencies up to sub-THz range [15].

Future developments consist of replacing the programmable discrete optical filter with SiP integrated optical filters for the selection of the comb modes as in [14]-[16], and replacing the optoelectronic modulation and photo-detection stages with the use of a silicon integrated optoelectronic mixer, as in [18]. In this way, the entire photonic hardware responsible for the up conversion could be monolithically integrated on a silicon platform, so as to be embedded in a single optoelectronic package, so as to minimize footprint, weight and power consumption. In addition to single-carrier PSK and QAM modulation formats, transmission performance of orthogonal frequency-division multiplexing (OFDM) signals will be also investigated, to match the requirements of current and forthcoming 5G, B5G and 6G standards.

Acknowledgment

The Authors would like to thank Prof. Marco Secondini for constructive discussions on EVM measurement.

References

[1] Cerwall, P. et al., “Ericsson Mobility Report November 2021”, Ericsson Mobility Report 1–40, 2021

[2] S. Tripathi et al, "6G Mobile Wireless Networks", Springer (2021)

[3] X. You, CX. Wang, J. Huang et al. “Towards 6G wireless communication networks: vision, enabling technologies, and new paradigm shifts” Sci. China Inf. Sci. 64, 110301 (2021)

[4] “5G Evolution Toward 5G Advanced: An overview of 3GPP releases 17 and 18”, Ericsson Technology Review 14, 1–13, 2021

[5] von Butovitsch, P. et al., “Advanced antenna systems for 5G networks”, Ericsson white paper 1–15 (2018)

[6] Rubiola, E. & Boudot, R., “Phase noise in RF and microwave amplifiers”, 2010 IEEE International Frequency Control Symposium 109–111, 2010

[7] Sengupta, K., Nagatsuma, T. & Mittleman, D. M., “Terahertz integrated electronic and hybrid electronic–photonic systems”, Nature Electronics 1, 622–635, 2018

[8] Tetsumoto, T. et al., “Optically referenced 300 GHz millimitre-wave oscillator”, Nature Photonics 15 516–522, 2021

[9] A. Siligaris, Y. Andee, C. Jany, V. Puyal, J. M. Guerra, J.L.G. Jimenez, and P. Vincent, “A 270-to-300 GHz subharmonic injection locked oscillator for frequency synthesis in sub-mmW systems”. IEEE Microwave and Wireless Components Letters, vol. 25, no. 4, pp.259-261, 2015.

[10] A. J. Seeds, H. Shams, M. J. Fice, and C. C. Renaud, “Terahertz photonics for wireless communications”, Journal of Lightwave Technology, vol. 33, no. 3, pp. 579–587, 2015

[11] A. Delmade, C. Browning, T. Verolet, J. Poette, A. Farhang, H. H. Elwan, R. D. Koilpillai, G. Aubin, F. Lelarge, A. Ramdane, D. Venkitesh, and L. P. Barry, “Optical heterodyne analog radio-over-fiber link for millimeter-wave wireless systems”, Journal of Lightwave Technology, vol. 39, no. 2, pp. 465-474, 2020

[12] P.T. Dat, Y. Yamaguchi, M. Motoya, S. Oikawa, J. Ichikawa, A. Kanno, N. Yamamoto, and T. Kawanishi, “Transparent Fiber–Millimeter-Wave–Fiber System in 100-GHz Band Using Optical Modulator and Photonic Down-Conversion”, Journal of Lightwave Technology, vol. 40, no. 5, pp. 1483-1493, 2022,

[13] R. Guzmán, L. González, A. Zarzuelo, J. Cesar Cuello, M. Ali, I. Visscher, R. Grootjans, J. P. Epping, C.G. H. Roeloffzen, and G. Carpintero, “Widely Tunable RF Signal Generation Using an InP/Si3N4 Hybrid Integrated Dual-Wavelength Optical Heterodyne Source”, Journal of Lightwave Technology, vol. 39, no. 24, pp. 7664-7671, 2021

[14] A. Malacarne, A. Bigongiari, A. D'Errico, A. Bogoni and C. Porzi, "Reconfigurable Low Phase Noise RF Carrier Generation up to W-Band in Silicon Photonics Technology," in Journal of Lightwave Technology, vol. 40, no. 20, pp. 6891-6900, 15 Oct.15, 2022.

[15] C. Porzi, A. Malacarne, A. Bigongiari, A. D’Errico, A. Bogoni, “Silicon Photonics Programmable Millimeter-Wave Band RF Synthesizer”, accepted as oral presentation for oncoming ECOC2023, European Conference on Optical Communication, 2023

[16] C. Porzi, F. Falconi, M. Sorel and A. Bogoni, "Broadband and High-Capacity Silicon Photonics Single-Sideband Modulator," in Journal of Lightwave Technology, vol. 40, no. 2, pp. 538-546, 2022.

[17] F. Alimenti, P. Mezzanotte, L. Roselli, and R. Sorrentino, “Modeling and characterization of the bonding-wire interconnection,” IEEE Trans. Microw. Theory Tech., vol. 49, no. 1, pp. 142–150, 2001.

[18] A. Montanaro, G. Piccinini, V. Mišeikis et al., “Sub-THz wireless transmission based on graphene integrated optoelectronic mixer”, 03 August 2022, PREPRINT (Version 1) available at Research Square [https://doi.org/10.21203/rs.3.rs-1835036